

Sentinel-2 and Sentinel-3 Imagery for Estimating Actual Evapotranspiration in the Denguélé District (Côte d'Ivoire)

Cédric Arnaud INAGO^{1*}, Naga COULIBALY², Matogona CISSÉ¹, Euclide N'GORAN¹, Dramane YAO¹, Gaoussou SYLLA, Koffi Claude Alain KOUADIO³, Houébagnon Saint Jean Patrick COULIBALY¹, Souleymane CISSÉ¹, Kambiré SIÉ¹

¹Laboratoire de Géosciences et Environnement, UFR Science et Gestion de l'Environnement, Nangui Abrogoua Univer-sité, Abidjan, Côte d'Ivoire

²UFR Agriculture, Ressources Halieutiques Et Agro-Industrie, Université de San-Pedro, San-Pedro, Côte d'Ivoire

³Laboratoire de Mathématique-Physique-Chimie, UFR Sciences Biologique, Université Péléforo Gon Coulibaly, Korho-go, Côte d'Ivoire

DOI: <https://doi.org/10.36347/sjavs.2026.v13i05.001>

| Received: 05.04.2026 | Accepted: 26.05.2026 | Published: 02.06.2026

*Corresponding author: Cédric Arnaud INAGO

Laboratoire de Géosciences et Environnement, UFR Science et Gestion de l'Environnement, Nangui Abrogoua Univer-sité, Abidjan, Côte d'Ivoire

Abstract

Original Research Article

Actual evapotranspiration is a key parameter for the water balance, crop water requirements and hydrological forecasting. It is therefore very important to understand this parameter in order to comprehend water balance phenomena and manage water resources. Furthermore, remote sensing has proven to be a useful tool for estimating this parameter, thanks to the accuracy and ease of access of this data. This study enabled us to estimate actual evapotranspiration in the Denguélé district using the SEBAL model and Sentinel imagery. Using this model, which is based on the energy balance, the aim of this study was to determine the net radiation, the ground heat flux and the sensible heat flux. Two dates were selected: 21 January 2018 (during the dry season) and 20 June 2018 (during the rainy season). The results for actual evapotranspiration vary depending on the vegetation cover. The highest values are observed in areas with dense vegetation (2.35 and 2.85 mm/day on 21 January 2018 and 6 and 6.52 mm/day on 20 June 2018), whilst areas of bare soil have lower evapotranspiration (between 1.15 and 2 mm/day on 21 January 2018 and between 4.5 and 5.33 mm/day on 20 June 2018). Although these estimates are of limited scope, the model used and the estimated climate parameters appear to hold considerable promise for effective application on a large scale.

Keywords: Evapotranspiration, SEBAL, Remote sensing, Denguélé District, Water demand.

Copyright © 2026 The Author(s): This is an open-access article distributed under the terms of the Creative Commons Attribution 4.0 International License (CC BY-NC 4.0) which permits unrestricted use, distribution, and reproduction in any medium for non-commercial use provided the original author and source are credited.

1. INTRODUCTION

In recent years, climate change has been causing significant disruptions. These include greater variability in rainfall and an increase in the frequency of extreme weather events such as floods, droughts, cyclones, tsunamis, etc. (IPCC, 2008). Globally, statistics show that during the 20th century, the Earth has warmed by 0.76°C (Chebil *et al.*, 2011). All of this has an impact on the environment and on all sectors of activity, particularly agriculture. Not only is agriculture the world's primary source of food, but it is also a sector that is heavily dependent on the availability of water, accounting for over 70% of freshwater use. To feed a global population expected to reach around 9 billion people by 2050, agricultural production will need to increase by around 50%, which will lead to a 15% rise in water abstraction. Today, more than ever before, the irrigated agriculture sector recognises the need to make

optimal use of water resources. Consequently, the benefits of rational irrigation water management are now well established (Hamimed *et al.*, 2001). It is therefore necessary to use appropriate techniques to assess crop water requirements in a simple, accurate and continuous manner.

Among these techniques, remote sensing is now regarded as an indispensable method. Indeed, it has become widely adopted due to its holistic view of environmental phenomena and its low cost compared to conventional methods based on in situ observations (Khellouk *et al.*, 2020). In the atmosphere, energy and water exchanges are key variables for hydrology, meteorology and, above all, agronomy (Ludwig & Mauser, 2000; Chen & Dudhia, 2001; Olioso *et al.*, 2002). Diarra (2017) explains that it is this understanding of the physics of these interactions, their dynamics and

their representation within modelling tools that has enabled remote sensing to better understand evapotranspiration or latent heat flux. In addition to playing a key role in the thermo-hydrological functioning of vegetation cover, evapotranspiration is closely linked to the productivity of agricultural and natural systems, as it lies at the heart of the processes of photosynthesis and water use by plants. Its observation and the development of numerical modelling tools have been intensified over recent decades with the aim of assessing water resource availability (Pitman, 2003).

There are several methods for determining potential or maximum evapotranspiration. Potential evapotranspiration is incorporated into a number of hydrological and agricultural simulation models, notably models such as CropWat and AquaCrop for crop models, and hydrological models such as SWAT, particularly via the Penman and Monteith, Priestley and Taylor, and Hargreaves (Hargreaves et Allen, 2003 ; Monteith, 1972 ; Penman, 1948 ; Priestley et Taylor, 1972) . However, when assessing a plant's water requirements, it is important to take into account climatic fluctuations and the specific characteristics of the plant. It is in this context that actual or effective evapotranspiration comes into play; this represents the quantity of water vapour actually released into the atmosphere from the soil and vegetation when the surface is at its natural moisture content, taking into account the actual water constraints of the site.

Numerous theories and approaches based on remote sensing have been developed to estimate actual evapotranspiration. In particular, models based on energy balance analysis, such as the SEBAL model (Bastiaanssen *et al*, 1998) . This model is suitable for estimating evapotranspiration over large areas, using high-temporal-resolution multispectral satellite imagery. It is within this context that this study is situated, the objective of which is to estimate actual evapotranspiration over a large area using Sentinel-2 and Sentinel-3 imagery in the Denguélé district.

2. MATERIAL AND METHODS

2.1. Study area

The Denguélé district, located in north-western Côte d'Ivoire, lies more precisely between latitudes 8° 30'43" and 10° 27'34" North and longitudes 8° 09'33" and 6° 35'10" West. Covering an area of approximately 20,600 km², it has an estimated population of 436,015 inhabitants according to the National Institute of Statistics (INS, 2021). This district borders the Savanes and Woroba districts to the east and south respectively, Mali to the north and Guinea to the west. The district capital is Odienné.

The geomorphology of the study area allows us to distinguish between two distinct parts. The western part comprises a fairly extensive plateau at altitudes of

between 400 and 450 metres, whilst in the east, altitudes generally exceed 500 metres and the plateaus are more rugged. With regard to soil science, the soils in this part of the West African craton belong, according to the terminology of the French soil classification system, to the ferrallitic soil class in the southern part and to the ferruginous soil class in the far north (Fileron, 1995) .

The Denguélé region has a humid tropical climate, characterised by two seasons (wet and dry), with an average annual rainfall of between 1,100 mm and 1,600 mm. The wet season runs from May to September and the dry season lasts seven months, marked by long periods of the Harmattan (December, January and February) (Fileron, 1995) .

The region is heavily forested where it has not been converted to agricultural land, with savannahs of the 'open forest' type.

2.2. Material

Satellite data

Sentinel images

The Sentinel-2 images used in our study are Level 2 images, with cloud cover of less than 10%. Eight scenes enabled us to cover the entire Denguélé District. These are scenes T29PNL, T29PNM, T29PPK, T29PPL, T29PPM, T29PQK, T29PQL and T29PQM from 21 January 2018 and 20 June 2018. These images were obtained from the Copernicus Browser website (<https://browser.dataspace.copernicus.eu/>) provided by the European Space Agency (ESA). The Sentinel-3 images used in this study are SLSTR images also dated 21 January 2018 and 20 June 2018. These images provide daily ground temperature with a resolution of 1 km. For this study, Sentinel-2 and Sentinel-3 images were used to determine actual daily evapotranspiration during the dry season and the rainy season.

SYN1deg data

The SYN1deg products are a dataset from NASA's CERES (Clouds and the Earth's Radiant Energy System) programme. Designed to provide radiative fluxes at the Earth's surface with a three-hourly temporal resolution and a spatial resolution of 1° x 1°, it incorporates data from geostationary satellites, enabling explicit tracking of the diurnal cycle of clouds and radiation. SYN1deg products are available on the project website (<https://ceres.larc.nasa.gov/>). These include, in particular, short-wave radiation, long-wave radiation and net flux. Using data from 21 and 23 January, 20 June and 30 September 2018, we determined the daily net radiation for our study area.

Climate data

For the purposes of our study, we used the following AgERA5 climate data: wind speed, air temperature at 2 m, relative humidity and surface pressure. This data comes from the Copernicus 'Climate Data Store' (<https://cds.climate.copernicus.eu/>), which

provides daily meteorological data for the period from 1979 to the present day, intended for agricultural and agroecological studies. The data used in this study to

determine evapotranspiration are those for 21 January, 23 January and 20 June 2018.

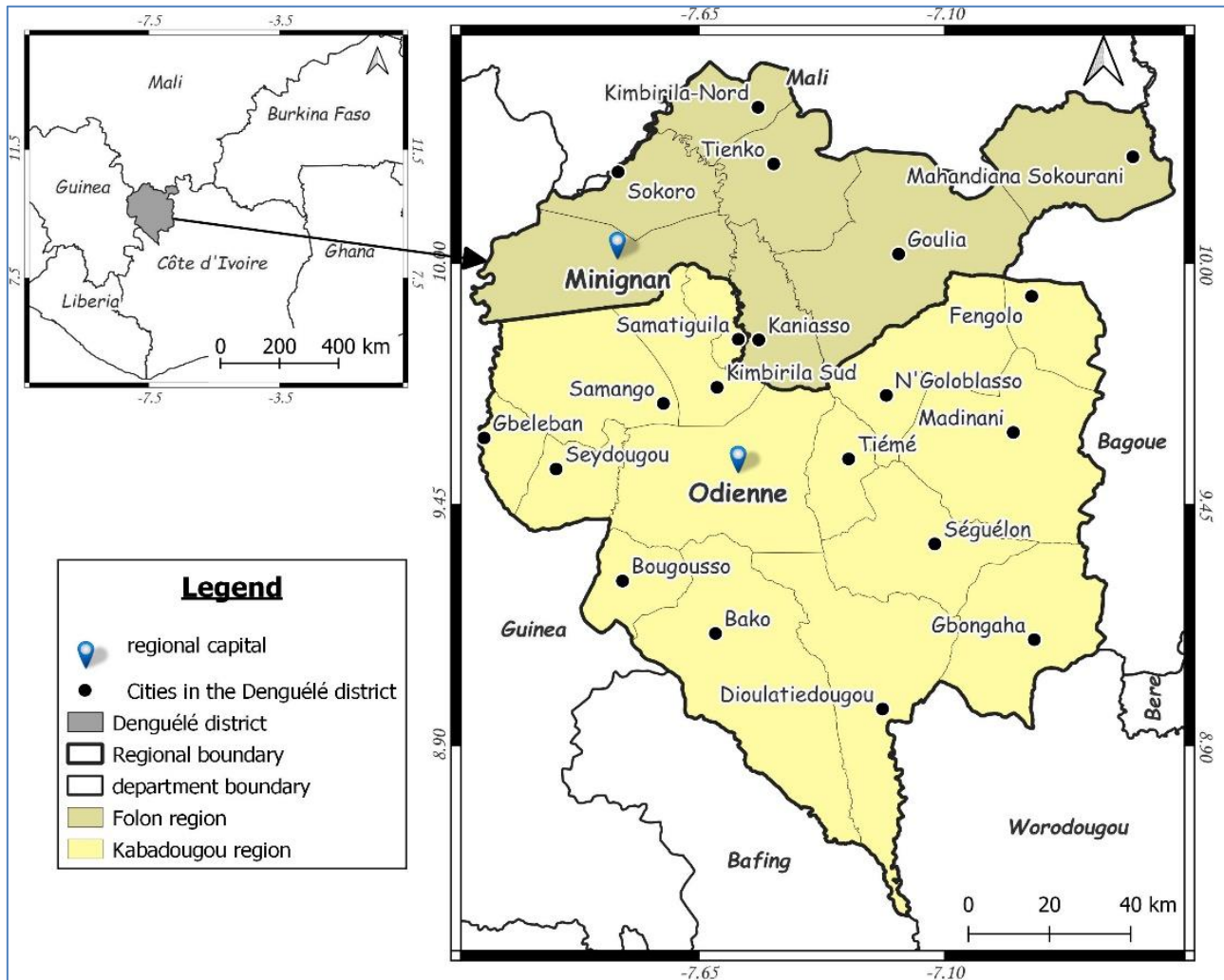


Figure 1: Location of the Denguélé district

2.3. Methods

The actual daily evapotranspiration was estimated using the SEBAL (Surface Energy Balance Algorithm for Land) model. This model is based on the solution to the energy balance equation developed by Bastiaanssen *et al.*, (1998).

$$R_n = LE + G + H \quad (\text{eq. 1})$$

Where R_n corresponds to the net radiation at ground level (W/m^2); G represents the ground heat flux (W/m^2); H represents the sensible heat flux (W/m^2) and LE represents the latent heat flux (W/m^2).

Evapotranspiration corresponds to the latent heat flux (LE) term in the energy balance (Courault *et al.*, 2005 ; Wassenaar *et al.*, 2002). Thus, in the SEBAL model, as in most models, LE is determined as the residual term in the energy balance equation.

Surface energy balance resolution

The net radiation at the ground surface

R_n is calculated by subtracting all outgoing radiative fluxes from all incoming radiative fluxes and includes solar and thermal radiation (Allen *et al*, 2007).

$$R_n = (1 - \alpha)R_{S\downarrow} + R_{L\downarrow} - R_{L\uparrow} - (1 - \epsilon_0)R_{L\downarrow} \quad (\text{eq. 2})$$

where $R_{S\downarrow}$ = incoming short-wave radiation ($W \cdot m^{-2}$); α = dimensionless surface albedo; $R_{L\downarrow}$ = incoming long-wave radiation ($W \cdot m^{-2}$); $R_{L\uparrow}$ = outgoing long-wave radiation ($W \cdot m^{-2}$) and ϵ_0 = dimensionless broadband thermal emissivity of the surface. The term $(1 - \epsilon_0)R_{L\downarrow}$ represents the fraction of incoming long-wave radiation reflected by the surface.

As for albedo, it is defined as the ratio of solar energy reflected by a surface to incident solar energy (Kyalo, 2017).

$$\alpha = 0.356 * b_1 + 0.13 * b_3 + 0.373 * b_4 + 0.085 * b_5 + 0.072 * b_7 - 0.0018 \quad (\text{eq. 3})$$

Where b_1 , b_3 , b_4 , b_5 , and b_7 represent the different spectral bands of Sentinel-2.

Ground heat flux

Heat transfer by conduction refers to the propagation of heat from molecule to molecule within one or more contiguous, opaque, solid bodies. Based on Fourier's law, soil heat flux is the rate at which heat is stored in the soil and vegetation due to conduction (Bastiaanssen, 2000) and is expressed by the following equation.

$$G = (LST - 273,15)(0,0038 + 0,0074\alpha) \times (1 - 0,978 \times NDVI^4) \times Rn \quad (\text{eq.4})$$

where LST = surface temperature in K derived from the Landsat 8 OLI image, and α = surface albedo.

Sensible heat flux

Convective heat transfer refers to the transfer of energy or mass through the movement of air between the surface and the lower layers of the atmosphere. The energy fluxes resulting from convective exchange are the momentum flux τ , the sensible heat flux H and the latent heat flux LE. The sensible heat flux H is expressed as a function of the difference between a temperature at a theoretical height within the canopy (the aerodynamic temperature) and the air temperature (Awad, 2019) .

$$H = \rho C_p \frac{T_a - LST}{r_H} \quad (\text{eq. 5})$$

H is the sensible heat flux in $W \cdot m^{-2}$, T_a and T_s are the air and surface temperatures in ($^{\circ}C$), r is the air density ($kg \cdot m^{-3}$) and C_p is the specific heat capacity of air, ($kJ \cdot kg^{-1}$) are constants, and r_H is the heat transfer resistance ($s \cdot m^{-1}$), which depends on wind speed and surface characteristics.

Actual evapotranspiration

The daily ET_a (*Actual Evapotranspiration*) value is calculated from the latent heat flux (LE) according to (Shu *et al.*, 2006) using the following equation.

$$ET_a = 86400 * EF * (R_{n24} - G_{24}) / \lambda \quad (\text{eq. 6})$$

- Where: $EF = LE / (Rn - G)$ Evaporation fraction;
- ET_0 Reference or potential evapotranspiration (mm/day) and
- $\lambda = [2,501 - (Ts - 273) * 0,002361] * 10^6$

3. RESULTS AND DISCUSSION

3.1. Results

Determination of Surface Indices

The vegetation indices obtained in the Denguélé District show the highest values in the southern and central parts during both the dry and rainy seasons. The highest values are particularly observed between Bako and Dioulatiédougou. The lowest values are recorded in the northern part of the district, especially in Kimbirila-Nord, Tienko, and Sokoro.

The land surface temperatures derived from Sentinel-2 images range from 304 to 310 K on 21/01/2018 and from 294 to 303 K on 20/06/2018. Despite the temperature differences between the two dates, with lower temperatures during the rainy season, a similar spatial variation is observed for both periods. It was also noted that temperature is inversely proportional to NDVI. Indeed, the lowest temperature values are observed in areas with denser vegetation cover, and vice versa.

Low albedo values are observed in areas with dense vegetation cover, whereas high values are found in moderately covered areas and bare soils. In addition, albedo values are lower during the rainy season than during the dry season.

Energy Balance Parameters

The net radiation (R_n) maps show a strong variation between the dry and rainy seasons (January and June). Indeed, the net radiation determined using the SEBAL model and Sentinel-2 images presents values ranging from 375 to 510 $W \cdot m^{-2}$ and from 525 to 625 $W \cdot m^{-2}$ for 21/01/2018 and 20/06/2018, respectively (Figure 2). Despite these differences, the trends and spatial distribution of radiation remain similar, as observed for the previous parameters.

The obtained soil heat flux results range between 78 and 90 $W \cdot m^{-2}$ on 21/01/2018 and between 78 and 100 $W \cdot m^{-2}$ on 20/06/2018. It can be observed that soil heat flux increases with vegetation density. Furthermore, the values are much lower during the rainy season.

The sensible heat flux shows a variation ranging from 90 to 205 $W \cdot m^{-2}$, with an average of 120 $W \cdot m^{-2}$ during the dry season, and from -45 to 60 $W \cdot m^{-2}$, with an average of 5.24 $W \cdot m^{-2}$ during the rainy season. The highest values are generally observed in areas where vegetation is less dense, whereas the lowest values are recorded in areas with high vegetation density.

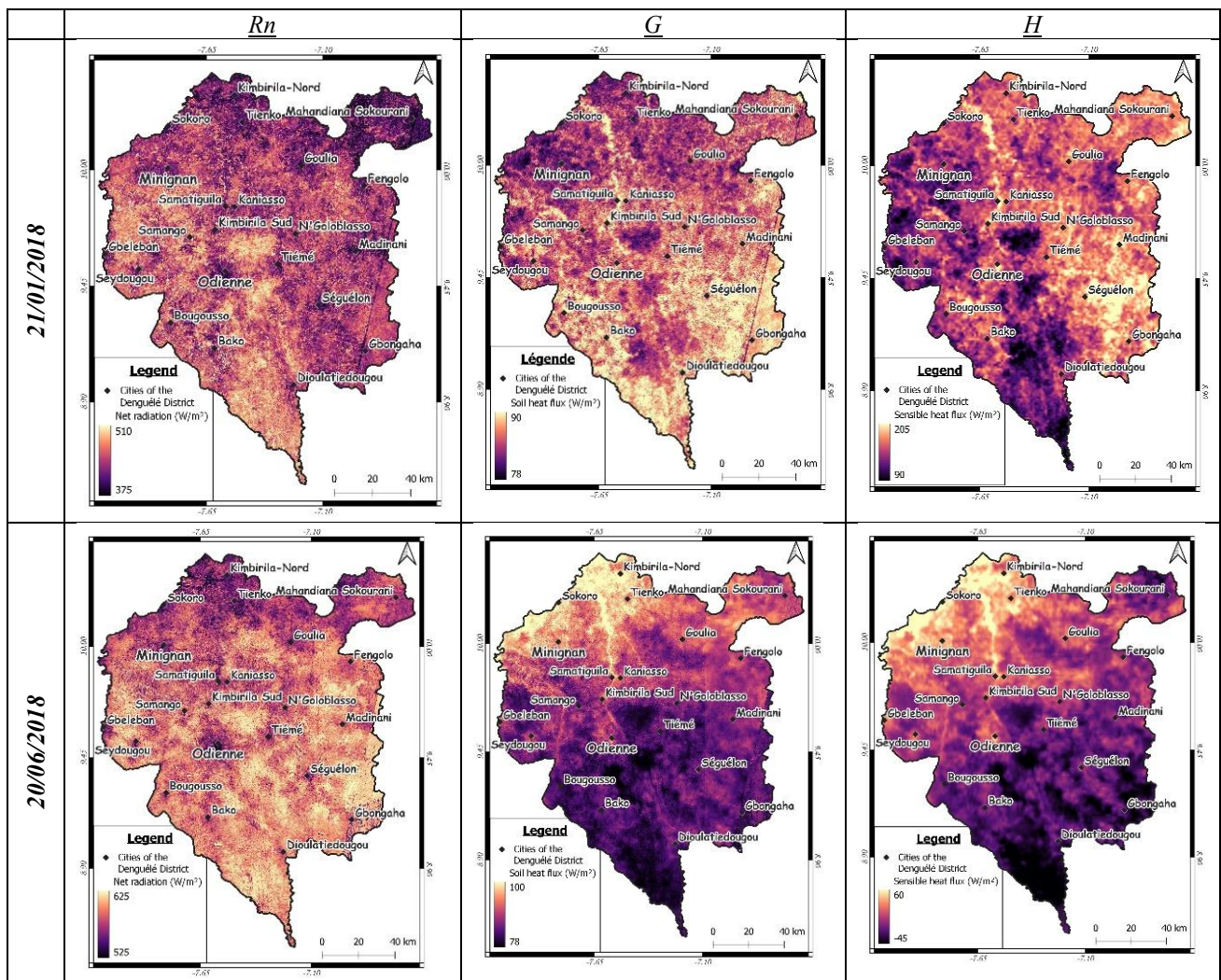


Figure 2: Energy balance parameters

Actual Evapotranspiration

After combining the results obtained from net radiation and sensible and latent heat fluxes, daily actual evapotranspiration was estimated (Figure 3). The results range from 1.15 to 3 mm/day, with an average of 1.89 mm/day on January 21, 2018, and from 4.5 to 6.75 mm/day, with an average of 5.6 mm/day on June 20, 2018.

High evapotranspiration values are observed in areas with high vegetation density, corresponding to higher NDVI values and lower albedo values, whereas low values are associated with bare soils and grass savanna areas, which correspond to lower NDVI values and higher albedo values.

Indeed, the area located between Odienné, Tiémé, Kimbirila-Sud, and N’Goloblasso, during both the dry and rainy seasons, shows above-average values ranging between 2.35 and 2.85 mm/day during the dry season and between 6 and 6.52 mm/day during the rainy season. The highest values are concentrated in the southern part, between the towns of Dioulatiédougou and Bako, where actual evapotranspiration reaches the maximum values of the district.

However, the northern and eastern areas show the lowest evapotranspiration values, with values recorded on January 21 and June 20, 2018, respectively, of 1.76 and 4.86 mm/day in Sokoro, 1.89 and 5.33 mm/day in Tienko, and 1.88 and 5.25 mm/day in Minignan.

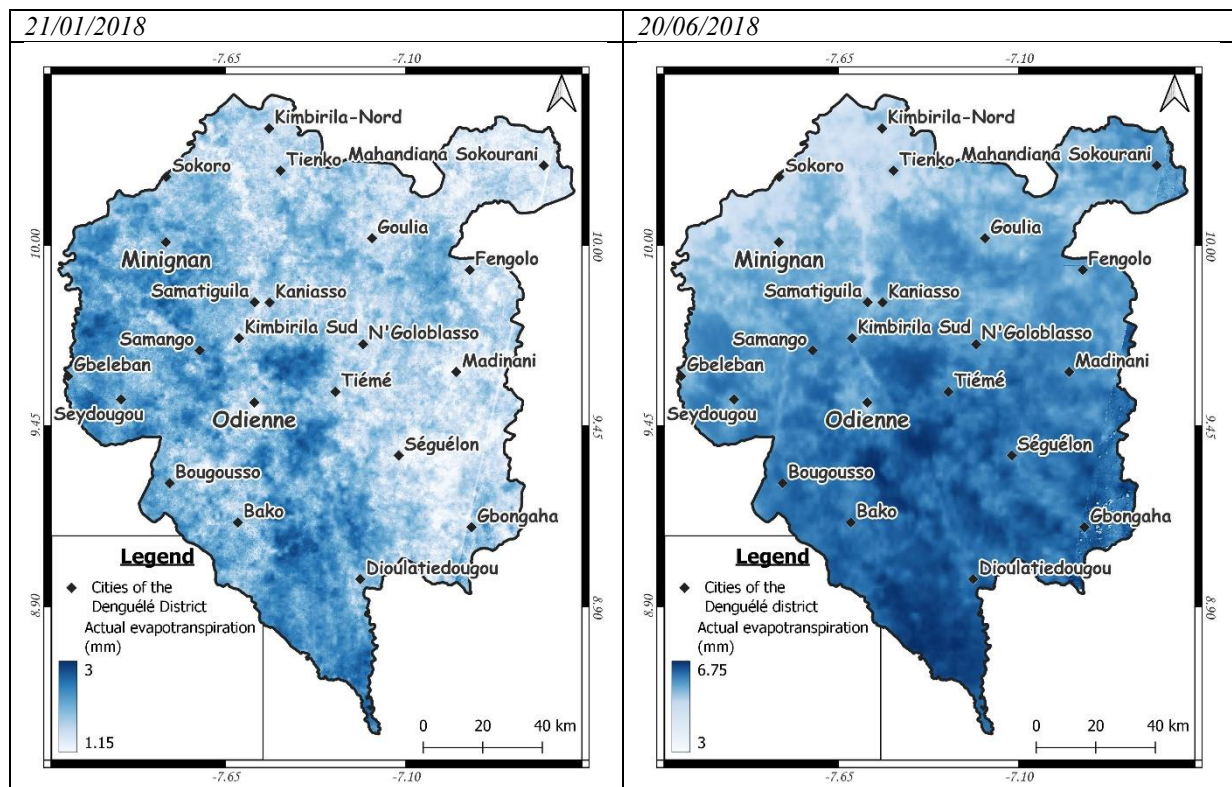


Figure 3: Actual Evapotranspiration

3.2. Discussion

The actual evapotranspiration values obtained in this study range from 1.15 to 3 mm/day during the dry season and from 4.5 to 6.75 mm/day during the rainy season. As can be observed, the highest values were recorded during the rainy season. This can be explained by water availability and the high vegetation activity during this period.

Similar results were obtained by Kra *et al.*, (2023) in 2019 in Yamoussoukro, central Côte d'Ivoire, with evapotranspiration ranging from 1.96 to 3.5 mm on December 19 and from 2.04 to 4.33 mm on February 15 using the SEBAL model with Landsat 8 imagery. This was also demonstrated in the forest-savanna transition zones of the Amazon, where the application of the SEBAL model produced actual evapotranspiration values of 4.2 mm/day in forests, while pasturelands and agricultural areas showed values between 2 and 3.2 mm/day (Laipelt *et al.*, 2020).

The results of this study highlight the heterogeneous nature of the study area surfaces due to the spatial variation of evapotranspiration. It is also observed that evapotranspiration derived from the energy balance exhibits the same trends as net radiation and NDVI. As confirmed by Kra *et al.*, (2023), the highest evapotranspiration values are obtained over water bodies and densely vegetated areas, whereas the lowest values are observed over bare soils and built-up surfaces.

Research conducted by Wei *et al.*, (2022) showed that, when assessing actual evapotranspiration during the seasonal rice growth cycle, the application of the SEBAL model demonstrated good accuracy ($R^2 = 0.82$, RMSE = 0.84 mm/day), which confirms the robustness of the SEBAL model.

5. CONCLUSION

This study demonstrated the value of Sentinel-2 and Sentinel-3 imagery combined with the SEBAL model for estimating actual evapotranspiration in the Denguélé district. The results highlight significant spatial and seasonal variability, with higher values in areas of dense vegetation and during the rainy season. These observations confirm the influence of vegetation cover and water availability on surface energy fluxes. Despite certain limitations related to climate data and biophysical characteristics, the approach adopted appears relevant for regional water monitoring and to support the sustainable management of water resources. Nevertheless, it should be noted that numerous climatic variables and plant characteristics, such as their form and growth stage, influence evapotranspiration.

REFERENCES

- Awad M. (2019). Toward Precision in Crop Yield Estimation Using Remote Sensing and Optimization Techniques. *Agriculture*, 9 (3), 54.
- Bastiaanssen W. G. M. (2000). SEBAL-based sensible and latent heat fluxes in the irrigated Gediz

- Basin, Turkey. *Journal of Hydrology*, 229 (1-2), 87-100.
- Bastiaanssen W. G. M., Menenti M., Feddes R. A., & Holtslag A. A. M. (1998). A remote sensing surface energy balance algorithm for land (SEBAL). 1. Formulation. *Journal of Hydrology*, 212-213, 198-212.
 - Chebil A., Mtimet N., Tizaoui H., & Chebil A. (2011). Impact du changement climatique sur la productivité des cultures céréalières dans la région de Béja (Tunisie). *African Journal of Agricultural and Resource Economics*, 6 (2), 1-11.
 - Courault D., Seguin B., & Olioso A. (2005). Review on estimation of evapotranspiration from remote sensing data: From empirical to numerical modeling approaches. *Irrigation and Drainage Systems*, 19 (3-4), 223-249.
 - Diarra A. (2017). Suivi de l'évapotranspiration des cultures irriguées du Sud de la Méditerranée par télédétection multi-capteurs et modélisation globale. Université Pierre et Marie Curie - Paris VI, France.
 - Fileron J.-C. (1995). Essai de géographie systématique : les paysages du Nord-Ouest de la Côte d'Ivoire (Doctorat). Université Toulouse le Mirail - Toulouse II, France.
 - IPCC (2008). 2007 Assessment of Changes : Contribution of Climate Working Groups I, II and III to the Fourth Assessment Report of the Intergovernmental Panel on Climate Change [Core Drafting Team], Pachauri, R.K. et Reisinger, A. (publié sous la direction de~). GIEC. Genève, Suisse, 103 p.
 - Hamimed A., Mederbal K., & Khadi A. (2001). Utilisation des données satellitaires TM de Landsat pour le suivi de l'état hydrique d'un couvert végétal dans les conditions semi-arides en Algérie. *Revue Télédétection*, 2 (1), 29-38.
 - Hargreaves G. H., & Allen R. G. (2003). History and Evaluation of Hargreaves Evapotranspiration Equation. *Journal of Irrigation and Drainage Engineering*, 129 (1), 53-63.
 - INS (2021). Recensement Général de la Population et de l'Habitat. p. 37. INS-Institut National de la Statistique.
 - Khellouk R., Barakat A., Boudhar A., Hadria R., Lionboui H., El Jazouli A., Rais J., El Baghdadi M., & Benabdelouahab T. (2020). Spatiotemporal monitoring of surface soil moisture using optical remote sensing data: a case study in a semi-arid area. *Journal of Spatial Science*, 65 (3), 481-499.
 - Kra J. L., Adahi M. B., Konan-Waidhet B. A., N'Guessan J.-Y. K., Koné J. D., & Assidjo E. N. (2023). Estimation of the Actual Evapotranspiration by the SEBAL Method in the Irrigated Rice Perimeter of Zatta (Yamoussoukro—ôte d'Ivoire). *Journal of Water Resource and Protection*, 15 (10), 539-556.
 - Kyalo K. D. (2017). Sentinel-2 and Modis land surface temperature-based evapotranspiration for irrigation efficiency calculations (Mémoire de master). University of Twente, Pays-Bas.
 - Laipelt L., Ruhoff A. L., Fleischmann A. S., Kayser R. H. B., Kich E. D. M., Da Rocha H. R., & Neale C. M. U. (2020). Assessment of an Automated Calibration of the SEBAL Algorithm to Estimate Dry-Season Surface-Energy Partitioning in a Forest–Savanna Transition in Brazil. *Remote Sensing*, 12 (7), 1108.
 - Ludwig R., & Mauser W. (2000). Modelling catchment hydrology within a GIS based SVAT-model framework. *Hydrology and Earth System Sciences*, 4 (2), 239-249.
 - Monteith J. L. (1972). Solar Radiation and Productivity in Tropical Ecosystems. *The Journal of Applied Ecology*, 9 (3), 747.
 - Olioso A., Braud I., Chanzy A., Courault D., Demarty J., Kergoat L., Lewan E., Otléc C., Prévot L., Zhao W. G., Calvet J.-C., Cayrol P., Jongschaap R., Moulin S., Noilhan J., & Wigneron J.-P. (2002). SVAT modeling over the Alpilles-ReSeDA experiment : comparing SVAT models over wheat fields. *Agronomie*, 22 (6), 651-668.
 - Penman H. L. (1948). Natural evaporation from open water, bare soil and grass. *Proceedings of the Royal Society of London. Series A. Mathematical and Physical Sciences*, 193 (1032), 120-145.
 - Pitman A. J. (2003). The evolution of, and revolution in, land surface schemes designed for climate models. *International Journal of Climatology*, 23 (5), 479-510.
 - Priestley C. H. B., & Taylor R. J. (1972). On the Assessment of Surface Heat Flux and Evaporation Using Large-Scale Parameters. *Monthly Weather Review*, 100 (2), 81-92.
 - Shu Y., Lei Y., Zheng L., & Li H. (2006). A evapotranspiration (ET) model based GIS using LANDSAT data and MODIS data with improved resolution. In : M. Ehlers, U. Michel (Éd.). p. 63661N. Présenté à Remote Sensing, Stockholm, Sweden.
 - Wassenaar T., Olioso A., Hasager A., Jacob F., & Chehbouni A. (2002). Estimation of evapotranspiration on heterogeneous pixels. In : Proceedings of the First International Symposium on Recent Advances in Quantitative Remote Sensing. p. 458-465.
 - Wei G., Cao J., Xie H., Xie H., Yang Y., Wu C., Cui Y., & Luo Y. (2022). Spatial-Temporal Variation in Paddy Evapotranspiration in Subtropical Climate Regions Based on the SEBAL Model : A Case Study of the Ganfu Plain Irrigation System, Southern China. *Remote Sensing*, 14 (5), 1201.